Ascorbic Acid Deficiency Activates Cell Death and Disease Resistance Responses in Arabidopsis[1]

Valeria Pavet, Enrique Olmos[2], Guy Kiddle, Shaheen Mowla, Sanjay Kumar[3], John Antoniw, María E. Alvarez, and Christine H. Foyer*

Centro de Investigaciones en Química Biológica de Córdoba/Consejo Nacional de Investigaciones Científicas y Técnicas, Departamento de Química Biológica, Facultad de Ciencias Químicas, Universidad Nacional de Córdoba, Ciudad Universitaria, Cordoba 5000, Argentina (V.P., M.E.A.); and Crop Performance and Improvement Division (E.O., G.K., S.M., S.K., C.H.F.) and Wheat Pathogenesis Program, Plant-Pathogen Interactions Division (J.A.), Rothamsted Research, Harpenden, Hertfordshire AL5 2JQ, United Kingdom

Programmed cell death, developmental senescence, and responses to pathogens are linked through complex genetic controls that are influenced by redox regulation. Here we show that the Arabidopsis (*Arabidopsis thaliana*) low vitamin C mutants, *vtc1* and *vtc2*, which have between 10% and 25% of wild-type ascorbic acid, exhibit microlesions, express pathogenesis-related (PR) proteins, and have enhanced basal resistance against infections caused by *Pseudomonas syringae*. The mutants have a delayed senescence phenotype with smaller leaf cells than the wild type at maturity. The *vtc* leaves have more glutathione than the wild type, with higher ratios of reduced glutathione to glutathione disulfide. Expression of green fluorescence protein (GFP) fused to the nonexpressor of PR protein 1 (GFP-NPR1) was used to detect the presence of NPR1 in the nuclei of transformed plants. Fluorescence was observed in the nuclei of 6- to 8-week-old GFP-NPR1 *vtc1* plants, but not in the nuclei of transformed GFP-NPR1 wild-type plants at any developmental stage. The absence of senescence-associated gene 12 (SAG12) mRNA at the time when constitutive cell death and basal resistance were detected confirms that elaboration of innate immune responses in *vtc* plants does not result from activation of early senescence. Moreover, H_2O_2-sensitive genes are not induced at the time of systemic acquired resistance execution. These results demonstrate that ascorbic acid abundance modifies the threshold for activation of plant innate defense responses via redox mechanisms that are independent of the natural senescence program.

The complex relationships between programmed cell death (PCD) and natural senescence observed during leaf development are far from understood. However, one clear distinction is that senescence in leaves is essentially reversible, but PCD is not (Thomas et al., 2003). The genetically programmed cell suicide events that comprise PCD are triggered by enhanced levels of reactive oxygen species (ROS; Chen and Dickman, 2004; Laloi et al., 2004; Wagner et al., 2004). However, senescence-enhanced genes are also expressed in response to ROS (Navabpour et al., 2003).

While the chemical nature of ROS dictates that they are potentially harmful to cells, plants use ROS as second messengers in signal transduction cascades regulating diverse processes such as mitosis, tropisms, and cell death. It is now well accepted that ROS accumulation is crucial to plant development as well as defense (Foyer and Noctor, 2005a). ROS signal transduction will ensue only if ROS escape destruction by cellular antioxidants that determine the lifetime and specificity of the signal. Ascorbic acid (AA) and glutathione are the major redox buffers of the plant cells, and they themselves are also signal-transducing molecules that can either signal independently or further transmit ROS signals (Fig. 1). They are thus intrinsic to redox homeostasis and redox-signaling events (Foyer and Noctor, 2005b).

ROS production is often genetically programmed, for example, during the hypersensitive response (HR) and PCD following pathogen recognition (Jabs et al., 1996; Levine et al., 1996). In mammals, the mitochondria-controlled PCD response involves the proapoptotic Bax family of proteins and antiapoptotic Bcl-2 and Bcl-XL families. Although Bax, Bcl-2, and Bcl-XL homologs

[1] This work was supported by the Biotechnology and Biological Sciences Research Council (C.F., G.K., and J.A.); grants from Agencia Nacional de Promoción Científica y Tecnológica (BID 1201/OC–AR PICT 01–10123) and Fundación Antorchas and Secretaria de Ciencia y Tecnologia/Universidad Nacional de Córdoba (to M.E.A.); the Department of Biotechnology, Government of India, for a Biotechnology Overseas Associateship Award (to S.K.); the Royal Society (U.K.) for a short-term fellowship (to S.M.); CONICET for a fellowship (to V.P.); and the Spanish Government for a Mobility Grant of Researcher, Ministerio de Educacion y Ciencia (PR2004–0361; to E.O.).

[2] Present address: Centro de Edafologia y Biologia Aplicada del Segura/Consejo Superior de Investigaciones Científicas, Department of Plant Physiology, P.O. Box 164, 30080 Murcia, Spain.

[3] Present address: Biotechnology Division, Institute of Himalayan Bioresource Technology, P.O. Box 6, Palampur–176 061 (HP), India.

* Corresponding author; e-mail christine.foyer@bbsrc.ac.uk; fax 0044–1582–763010.

The authors responsible for distribution of materials integral to the findings presented in this article in accordance with the policy described in the Instructions for Authors (www.plantphysiol.org) are: Christine H. Foyer (christine.foyer@bbsrc.ac.uk) and María E. Alvarez (malena@mail.fcq.unc.edu.ar).

Article, publication date, and citation information can be found at www.plantphysiol.org/cgi/doi/10.1104/pp.105.067686.

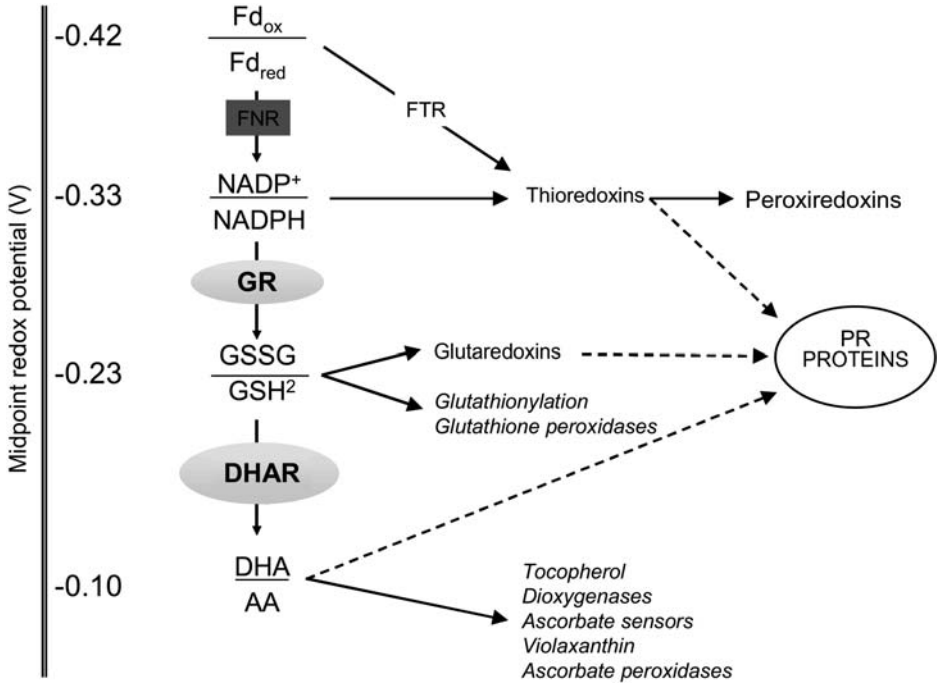

Figure 1. The involvement of key redox couples in the expression of PR proteins in plant cells. The major soluble reductant couples are arranged according to their midpoint potentials, with principal protein components with which they interact indicated. DHAR, Dehydroascorbate reductase; Fd_{ox}, oxidized ferredoxin; Fd_{red}, reduced ferredoxin; FTR, ferredoxin-thioredoxin reductase; GR, glutathione reductase. Solid arrows indicate known interactions, while broken arrows indicate putative components or redox couples implicated in the signal transduction cascade.

have not yet been found in plants, expression of mammalian Bax causes death, while that of mammalian Bcl-XL or Bl-1 suppresses cell death in plant cells challenged with elicitors, suggesting that elements of mammalian PCD processes are also found in plants (Matsumura et al., 2003). Moreover, mammalian Bcl-2 family proteins localize to the mitochondrial, chloroplast, and nuclear fractions when expressed in plants, where they prevent herbicide and ROS-induced PCD (Chen and Dickman, 2004). Such observations suggest that mitochondrial and chloroplast ROS accumulation is intrinsic to genetically programmed PCD events and function alongside NADPH oxidases and other superoxide-generating systems on the plasma membrane. Mitochondria also contribute to ROS-dependent gene expression during pathogen-induced PCD (Maxwell et al., 2002).

In addition to redox buffering and ROS detoxification (Foyer and Noctor, 2005a, 2005b), AA fulfills many essential roles in plant biology (Arrigoni and de Tullio, 2000). In particular, AA modulates growth through regulation of the cell cycle (Potters et al., 2002, 2004) and through regulation of elongation growth (Fry, 1998; Tokuna et al., 2005). AA and hydroxyl radicals participate in the oxidative scission of structural polysaccharides, promoting cell wall loosening (Fry, 1998). In addition, AA is a substrate for secretory peroxidases involved in cell wall stiffening and its presence limits the formation of phenolic radical intermediates in wall peroxidase reactions (de Pinto and De Gara, 2004).

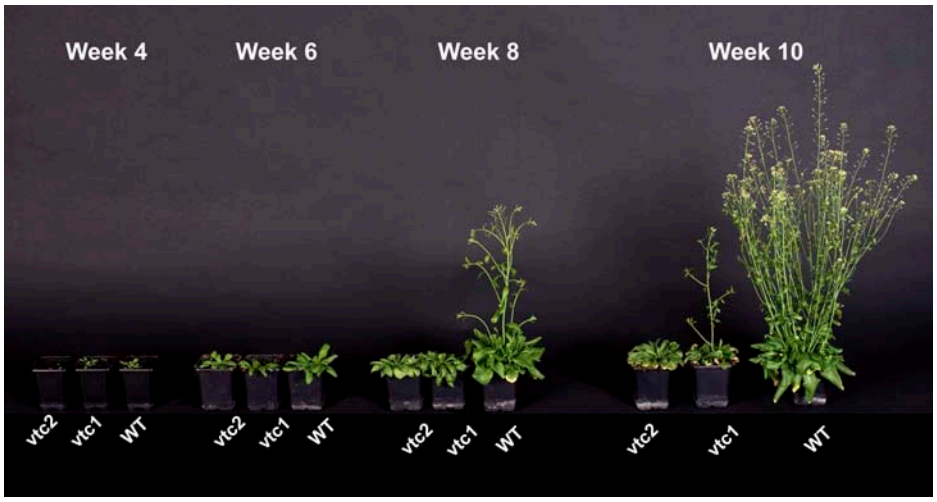

Figure 2. The delayed development phenotype of the *vtc1* (vtc1) and *vtc2* (vtc2) mutants compared to the wild type (WT). The number of weeks after sowing is indicated.

Table I. *Comparative developmental changes in vtc1-1, vtc2-1, and wild-type shoot biomass, leaf antioxidants, chlorophyll, and soluble protein*
FW, Fresh weight.

Plant Age	Biomass	GSH	Glutathione-Disulfide	GSH-to-GSSG Ratio	AA	Chlorophyll	Protein
	$g^{-1}FW$	$nmol\ g^{-1}\ FW$	$nmol\ g^{-1}\ FW$		$nmol\ g^{-1}\ FW$	$\mu g\ g^{-1}\ FW$	$mg^{-1}\ FW$
Week 2							
vtc2-1	0.004 ± 0.0002	235 ± 12	27 ± 1	9:1	624 ± 21	1,287 ± 29	11 (±0.4)
vtc1-1	0.003 ± 0.0001	368 ± 25	11 ± 1	33:1	1,154 ± 54	921 ± 13	13 (±0.3)
Col-0	0.006 ± 0.0003	272 ± 45	17 ± 3	16:1	3,395 ± 57	1,064 ± 12	13 (±0.5)
Week 4							
vtc2-1	0.09 ± 0.01	598 ± 20	37 ± 0.7	16:1	1,037 ± 67	1,186 ± 11	10 (±0.3)
vtc1-1	0.31 ± 0.01	546 ± 16	8 ± 0.5	68:1	1,278 ± 67	1,045 ± 7	9 (±0.2)
Col-0	0.52 ± 0.02	424 ± 31	13 ± 1	33:1	3,885 ± 100	894 ± 6	9 (±0.3)
Week 6							
vtc2-1	0.95 ± 0.15	338 ± 9	30 ± 2	11:1	639 ± 41	786 ± 15	9 (±0.2)
vtc1-1	1.17 ± 0.01	441 ± 16	8 ± 1	55:1	1,382 ± 43	970 ± 5	10 (±0.2)
Col-0	2.39 ± 0.08	326 ± 26	12 ± 3	27:1	4,648 ± 112	894 ± 6	10 (±0.4)
Week 8							
vtc2-1	4.62 ± 0.31	293 ± 10	9 ± 1	31:1	375 ± 26	996 ± 29	7 (±0.2)
vtc1-1	5.38 ± 0.12	312 ± 19	15 ± 1	20:1	1,464 ± 156	1,048 ± 10	9 (±0.3)
Col-0	8.03 ± 0.15	211 ± 16	17 ± 3	12:1	3,322 ± 123	895 ± 18	9 (±0.2)
Week 10							
vtc2-1	6.63 ± 0.14	279 ± 6	7 ± 1	60:1	–	1,073 ± 39	7 (±0.2)
vtc1-1	17.2 ± 0.12	298 ± 8	24 ± 4	12:1	–	1,146 ± 15	5 (±0.4)
Col-0	16.2 ± 0.11	183 ± 11	12 ± 2	15:1	–	680 ± 17	3 (±0.1)

AA-dependent dioxygenases participate in the synthetic pathways of a number of key plant hormones that also influence growth (Arrigoni and de Tullio, 2000). For example, AA is required for the activity of 9-cis-epoxycarotenoid dioxygenase, an enzyme catalyzing the formation of xanthoxin, the precursor of abscisic acid.

A number of Arabidopsis (*Arabidopsis thaliana*) mutants that have low AA (vitamin C; *vtc*) have been isolated (Conklin et al., 2000). Since the function of most of the genes modified in these mutants is unknown, we have concentrated our efforts on analyzing *vtc1* and *vtc2*, which are better characterized. Most importantly, the *vtc1* and *vtc2* phenotypes are caused by low AA alone, as shown by studies involving the expression of the animal AA biosynthetic enzyme L-gulono-1,4-oxidase, which restores wild-type AA levels and the wild-type phenotype to these mutants (Radzio et al., 2003). *vtc1* is relatively well studied, harboring a point mutation in the AA biosynthetic enzyme GDP-Man pyrophosphorylase (Conklin et al., 2000). This mutant was instrumental in the characterization of the pathway of AA synthesis in plants (Conklin et al., 1999). In contrast, *vtc2* (At4g26850) harbors a less-characterized mutation in an unknown protein (for gene database information, see, for example, http://mips.gsf.de/projects/plants).

The *vtc1* mutation confers sensitivity to ozone and other abiotic stresses, such as freezing and UV-B irradiation (Conklin et al., 1996), but it enhances pathogen resistance (Barth et al., 2004). We have previously

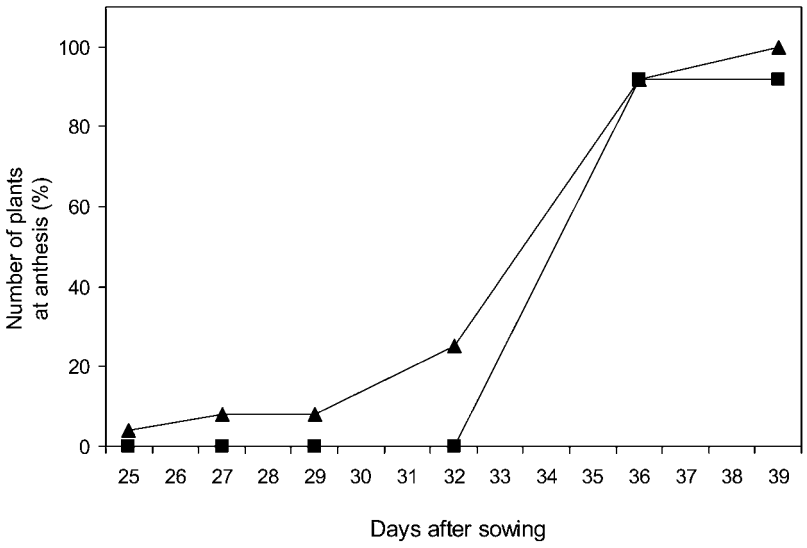

Figure 3. The appearance of the apical meristem is delayed in the *vtc1* mutant compared to the wild type. The days to flowering were compared in *vtc1* (■) and wild-type plants (▲). The experiment was performed using 100 plants and repeated three times with similar results.

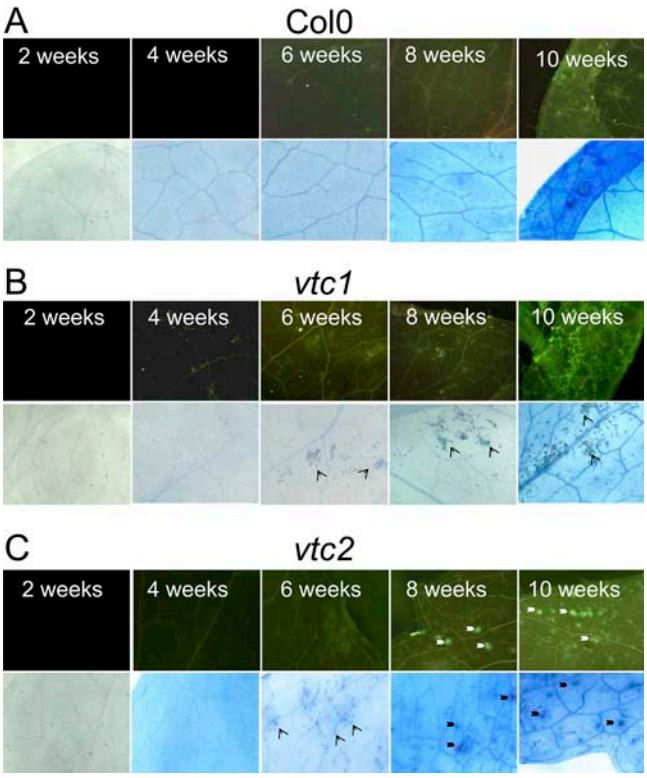

Figure 4. The appearance of individual dead cells (microlesions) in the rosette leaves of wild-type (A), *vtc1* (B), and *vtc2* (C) plants during development. Cell death was monitored using autofluorescence (top) or lactophenol blue staining (bottom) of leaf tissues. To aid clarity, examples of individual dead cells are marked with fine arrowheads, while large patches of dead cells are marked by thick arrowheads in the bottom images.

shown that AA deficiency in the *vtc1* mutant led to the differential expression of 171 genes, a substantial number of which encode pathogenesis-related (PR) proteins such as PR1, PR2, and PR5 (Kiddle et al., 2003; Pastori et al., 2003). Moreover, PR proteins accumulated more rapidly in *vtc1* than the wild type when challenged with *Pseudomonas syringae* (Barth et al., 2004). However, when grown under optimal growth conditions, *vtc1* shows no evident indications of increased oxidative stress in terms of tissue H_2O_2 content or the redox state of key indicator pools such as AA (Veljovic-Jovanovic et al., 2001).

Like AA (1–5 μmol mg^{-1} fresh weight or μmol mg^{-1} chlorophyll), glutathione is an abundant plant metabolite (100–300 nmol mg^{-1} fresh weight or nmol mg^{-1} chlorophyll) that has many diverse and important functions (Noctor and Foyer, 1998), including signal transduction (Noctor et al., 2002; Gomez et al., 2004). As an indicator of the general cellular thiol-disulfide redox balance, the reduced glutathione (GSH)-oxidized glutathione (GSSG) couple is well suited to the role of redox sensor. Cytosolic thiol-disulfide status appears to be important in regulating the expression of PR genes through the nonexpressor of PR protein 1 (NPR1) pathway (Mou et al., 2003). NPR1 is an intrinsic component of the salicylic acid (SA)-triggered systemic acquired resistance (SAR) response to biotic attack. The redox dependence of the NPR1 pathway implies that biotic or abiotic stimuli that perturb the cellular redox state can up-regulate defense genes via the NPR1 pathway (Mou et al., 2003). Such redox-linked effects explain, for example, PR gene expression in response to UV-B exposure (Green and Fluhr, 1995) and in catalase-deficient mutants (Chamnongpol et al., 1996). Figure 1 illustrates the redox relationships between the different components implicated in the regulation of NPR1 movement from the cytosol to the nucleus to elicit SAR and PR gene expression.

The redox poise of the plant cell at any moment in time is largely dictated by three redox pools, namely, pyridine nucleotides, AA, and glutathione (Fig. 1). The high cellular AA content dictates that it is the major low-M_r antioxidant and redox buffer of plant cells (Foyer, 2004). It is therefore logical to pose the question of whether low redox buffering capacity alone, as occurs during AA deficiency, is sufficient to trigger a redox-sensitive pathway leading to enhanced basal resistance. To address this question, we have analyzed SAR and pathogen resistance in two AA-deficient Arabidopsis mutants, *vtc1* and *vtc2*. We provide evidence that a decrease in overall cellular redox-buffering capacity in these mutants, resulting from a diminished AA pool, together with an enhanced GSH-to-GSSG ratio, reduces the threshold for local PCD and causes movement of NPR1 into the nucleus, triggering systemic resistance responses in the absence of enhanced ROS levels or external cues.

RESULTS

AA Deficiency Retards Growth and Senescence and Enhances Leaf GSH-to-GSSG Ratios

In this study, the Columbia (Col-0) wild type and the *vtc1* and *vtc2* mutants were grown in a 10-h photoperiod

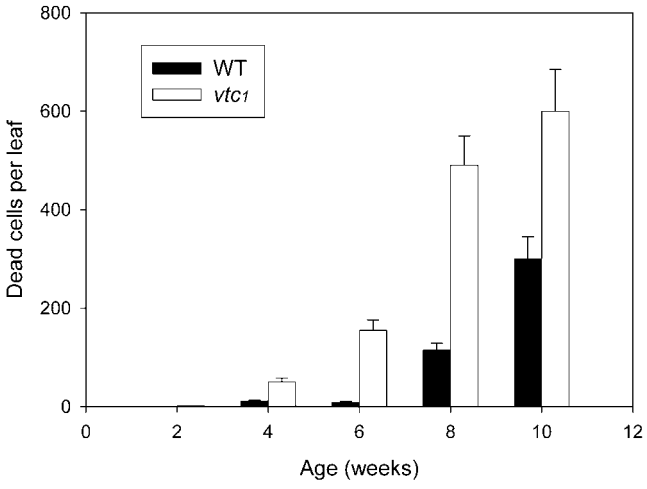

Figure 5. The number of dead cells present in *vtc1* and wild-type leaves through development. Values were calculated from leaves stained with lactophenol blue as shown in Figure 4, and data represent the means ± SE of five separate experiments involving 25 samples per line.

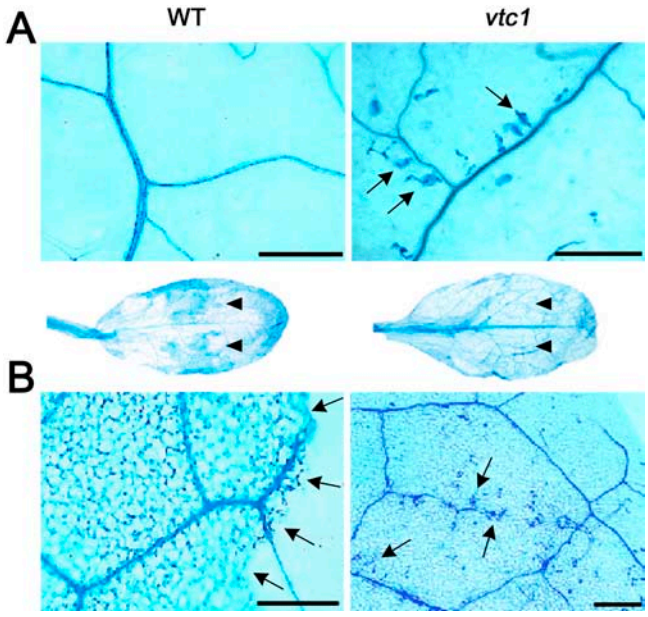

Figure 6. Pathogen-induced macroscopic and microscopic cell death symptoms are greatly decreased in *Pst*-infected *vtc1* leaves compared to *Pst*-infected wild-type leaves. A and B, Lactophenol blue staining of 7-week-old wild-type and *vtc1* leaves before (A) and after (B) pathogen inoculation (5×10^6 cfu/mL). The black arrows in A indicate the presence of individual dead cells in *vtc1* but not wild type (WT) in the absence of inoculation. Attached leaves were infiltrated with *Pst* at single-point sites (black arrowheads; B [top]), and pathogen-induced cell death was analyzed at 5 d postinfiltration. Middle section, The whole leaves show that patches of dead cells occur around inoculation sites in wild type but not in *vtc1*. Magnification of the infiltration sites (B [bottom]) shows massive cellular collapse (indicated by fat arrowheads) in the wild-type plants, whereas only a few small groups of dead cells in *vtc1* (thin arrows). Bars, 50 μm.

in controlled environment chambers with filtered air to remove atmospheric ozone. In these conditions, the *vtc1* (Fig. 2) and *vtc2* (data not shown; see Radzio et al., 2003) mutants were smaller at equivalent stages in development than wild-type plants. This phenotype was clearly evidenced at 2 weeks and was maintained throughout the plant growth cycle (Fig. 2). As shown in Table I, the *vtc1* and *vtc2* rosettes accumulate biomass at a much slower rate than the wild type. The *vtc1* leaves had about 70% less AA than the wild type throughout development. The *vtc2* mutants studied here had even lower leaf AA content for most of the growing period, with leaf AA reaching maximum values of about 25% of those of the wild type at 4 weeks (Table I). In addition, the *vtc1* leaves had 1.3 to 1.6 times more glutathione than the wild type. Moreover, the GSH-to-GSSG ratios of *vtc1* rosette leaves were almost double those measured in the wild type at all stages of development. The *vtc2* rosette leaves also tended to have more leaf glutathione than the wild type, with much higher GSH-to-GSSG ratios later in rosette development (Table I). Wild-type, *vtc1*, and *vtc2* leaves had similar amounts of chlorophyll and leaf protein at equivalent time points in the growth phase up to 10 weeks of growth. Thereafter, leaf chlorophyll and soluble protein declined in wild-type plants, but in *vtc1* and *vtc2* they remained at similar values to those observed at 8 weeks (Table I). On the other hand, the *vtc1* plants were delayed in flowering compared to the wild type (Fig. 3), as did *vtc2* (see Fig. 2). Together, these features show that *vtc1* and *vtc2* rosettes senesce later than the wild-type leaves.

Cell Death and Microscopic Lesions Are Evident in Naive *vtc1* Leaves from Early in Rosette Development

Macroscopic spontaneous lesions were not observed in naive *vtc1* leaves from plants grown on either short or long days (Fig. 2), but a few whole chlorotic leaves per plant appeared after 10 weeks, and these, by eye, might easily be mistaken for a symptom of senescence. However, in contrast to Col-0 rosette leaves (Fig. 4A), we consistently detected the presence of individual dead cells early in the development of *vtc1* (Fig. 4B) and *vtc2* (Fig. 4C) rosette leaves at the microscopic level. Small foci of collapsed cells were found all over the leaf surface and preferentially in the mesophyll layer of *vtc1* and *vtc2* leaves (Fig. 4, B and C). By 8 weeks, the areas of dead cells had expanded in *vtc2* leaves to form larger foci with clear patches of dead cells detectable by autofluorescence or lactophenol blue staining (Fig. 4C). Even the young (4–6 weeks) *vtc1* and *vtc2* rosettes had a small number of dead cells as detected by autofluorescence (Fig. 4, B and C) or lactophenol blue staining (Figs. 4 and 5). Individual dead cells were also detected in wild-type leaves, but their appearance was delayed compared to *vtc1* and *vtc2* (Figs. 4 and 5).

Enhanced Resistance to *P. syringae* Reveals That *vtc1* and *vtc2* Mutations Limit Bacterial Proliferation and Cell Death Expansion

To evaluate how *vtc1* controls cell death expansion once it is initiated by an exogenous stimulus, we challenged leaf tissues with high doses of the biotrophic bacterium *P. syringae* pv tomato DC3000 (*Pst*). This virulent pathogen proliferates in the intercellular spaces of leaf tissues of naive wild-type plants causing disease with spreading, chlorotic lesions (Whalen et al., 1991). However, proliferation is restricted when plants orchestrate SAR (Uknes et al., 1992; Cameron et al., 1994). We monitored the development of pathogen-induced lesions in 8-week-old wild-type and *vtc1* and *vtc2* plants infiltrated with a high titer of bacteria (5×10^6 cfu/mL). Large patches of necrotic tissue were evident 5 d postinfection in inoculated wild-type leaves, while only a few small groups of dead cells (without spreading necrosis) were found in inoculated *vtc1* tissues (Fig. 6). Thus, *vtc1* mutation does not lead to cell death propagation once it is initiated by *Pst* inoculation. Like *vtc1*, *vtc2* leaves exhibited individual collapsed cells in the young (4–6 weeks) rosettes. Spontaneous cell death is therefore more prolific in *vtc1* than *vtc2* leaves, whereas cell death patches were

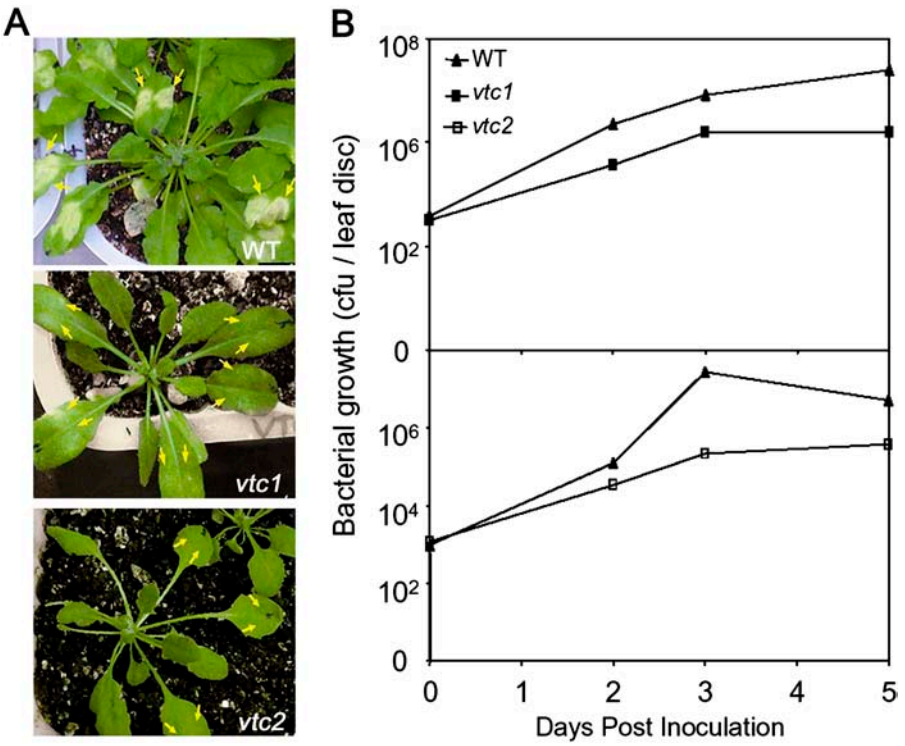

Figure 7. The *vtc1* and *vtc2* mutants display enhanced resistance to infection by *Pst*. Leaves from 6-week-old plants were locally infiltrated with *Pst* (5×10^6 cfu/mL), and symptoms were analyzed at the infiltration sites (indicated by yellow arrows) at 4 d postinfection. Visible disease symptoms, displayed by *Pst*-infected wild-type (Col-0) leaves, were much reduced in *vtc1* and *vtc2* plants (A). Moreover, *Pst* growth curves in planta, quantified in leaf discs excised at the indicated times from the infiltration sites inoculated with a low titer of *Pst* (10^5 cfu/mL), show that bacterial growth is restricted in *vtc1* and *vtc2* leaves compared with wild-type (Col-0) controls. Data represent the mean ± SE of three independent experiments (B).

more abundant in *vtc2* leaves in which AA content is much lower than *vtc1* at the 6- and 8-week stages (Table I). Individual dead cells were also detected in wild-type leaves, but their appearance was delayed compared to *vtc1* (Figs. 4 and 5).

Four days after *Pst* inoculation, typical disease symptoms were observed in wild-type leaves, while little chlorosis was detected in *vtc1* and *vtc2* leaves (Fig. 7A). We quantified bacterial growth in planta in wild type, *vtc1*, and *vtc2* infected tissues and observed that both mutations conferred the ability to restrict *Pst* proliferation by 15-fold and 13-fold, respectively, over wild-type levels (Fig. 7B). Similar protection is conferred by biological (Cameron et al., 1994) or chemical (Uknes et al., 1992; Alvarez et al. 1998) treatments activating SAR in wild-type plants. The level of basal resistance was measured every 2 to 3 weeks during the development of naive wild-type and *vtc1* plants. Enhanced levels of basal resistance were clearly detectable in *vtc1* plants at 6 to 8 weeks (Fig. 8).

The *vtc1* and *vtc2* Mutations Lead to Constitutive Expression of PR Genes But Not the Antioxidant *GST* Gene or Early Expression of the Senescence Marker Gene *SAG12*

By week 6, both mutants displayed constitutive expression of PR genes (Fig. 9). However, neither *vtc* mutants nor wild-type plants displayed substantial constitutive expression of the antioxidant glutathione *S*-transferase (*GST*) gene at this time (Fig. 9). PR gene expression was first detected in naive *vtc1* plants after 6 weeks of growth and was clearly evident by week 8 (Fig. 10). In contrast, PR expression was active only at the time of senescence in wild-type plants (about 16 weeks; Fig. 10). Neither Col-0 nor *vtc1* plants showed expression of the senescence marker gene senescence-associated gene 12 (*SAG12*) during the developmental period in which leaves were analyzed (2–11 weeks) in these experiments (Fig. 10). The absence of *SAG12* expression in *vtc1* confirms the

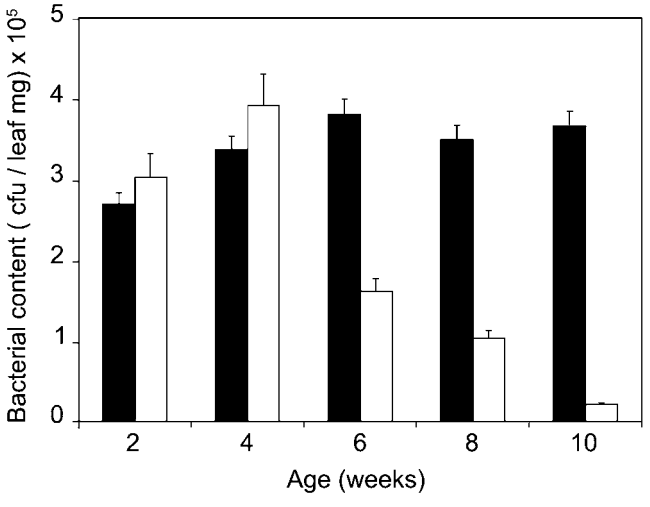

Figure 8. Growth of *Pst* is increasingly restricted as *vtc1* rosettes develop. Leaves from 2-, 4-, 6-, 8-, and 11-week-old plants were infiltrated with *Pst* (10^5 cfu/mL). *Pst* growth in planta was quantified in leaf discs excised from infiltration sites at 5 d postinfiltration. Data represent the mean ± SE of three independent experiments.

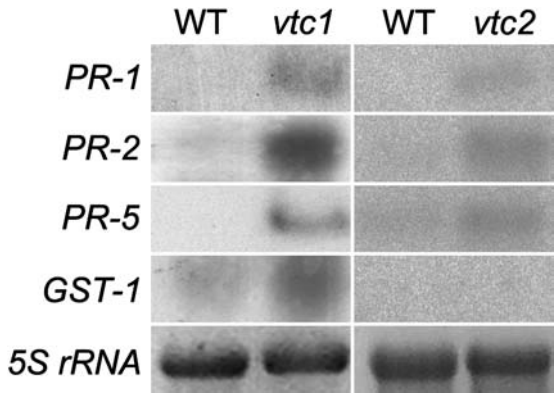

Figure 9. Six-week-old *vtc1* (left) and *vtc2* (right) rosette leaves constitutively express *PR* transcripts. RNA-blot analyses of wild-type, *vtc1*, and *vtc2* naive leaf tissues were hybridized with Arabidopsis probes (Uknes et al., 1992). The *5S rRNA* probe was used as the gel-loading control.

conclusion drawn from the enhanced duration of levels of high protein and chlorophyll that *vtc1* rosettes do not develop faster or senesce earlier than the wild-type plants.

The vtc1 and *vtc2* Mutations Lead Early Cessation of Cell Expansion Coupled to Movement of NPR1 into the Nucleus

The mature *vtc1* and *vtc2* leaves had the same numbers of cells as the wild type, but they were smaller (Fig. 11). The *vtc1* leaf cells stopped growing early in development at about week 6 (Fig. 12). Transgenic wild-type and *vtc1* plants expressing green fluorescent protein (GFP) fused to NPR1 (Col-0 GFP-NPR1 and *vtc1* GFP-NPR1, respectively) were constructed and the fluorescence profile was assessed throughout the development of homozygous transformed plants. The amount of GFP fluorescence observed in the cytosol of mesophyll or epidermal cells was very low in all conditions. However, the stomatal guard cells of all genotypes always showed nuclear localization of NPR1 as observed by high fluorescence (Fig. 13), as reported previously (Mou et al., 2003). When the fluorescence images are overlaid bright-field images of the cells (Fig. 14, bottom), then nuclear localization of the fluorescent spots within the guard cell pairs is evident. A higher resolution image of an individual stomatal guard cell pair is shown in the inset to Figure 14 (bottom right) to clearly illustrate this point.

GFP fluorescence was not detected in the nuclei of unchallenged mesophyll or epidermal cells of transgenic Col-0 plants at any stage of development (Figs. 13 and 14). However, GFP fluorescence accumulated in the nuclei of transgenic Col-0 plants following the application of SA (Fig. 13, bottom). Similarly, GFP fluorescence was not accumulated in the nuclei of unchallenged mesophyll or epidermal cells of transgenic *vtc1* rosettes prior to the 6-week stage. Thereafter, however, fluorescence increased in the nuclei of transgenic *vtc1* rosettes, becoming increasingly intense at 8 weeks and beyond (Fig. 14).

DISCUSSION

As in animals, plant PCD is a physiological process that is indispensable for correct development and regulates homeostasis through the elimination of unneeded cells. In contrast to necrosis, PCD is triggered by intrinsic factors or extrinsic defense cues and is executed through genetic signals that lead to a cell suicide program through the activation of defined autolytic processes. Current concepts suggest that pathogen-induced PCD is triggered by an interaction of signaling molecules, such as ROS and nitric oxide, and simultaneous suppression of ROS detoxification (Delledonne et al., 2001; Apel and Hirt, 2004). ROS-mediated cell suicide events are genetically controlled (Wagner et al., 2004) and ROS are required in many (but not all) systems leading to pathogen-induced PCD (Apel and Hirt, 2004). The intrinsic pathway involves two of the most important ROS-generating organelles of the plant cell, the chloroplasts and the mitochondria (Chen and Dickman, 2004; Yao et al., 2004). The aim of this study was to elucidate the mechanisms whereby AA deficiency in the *vtc1* and *vtc2* mutants modifies pathogen-induced PCD and enhances pathogen resistance. In addition, the experiments were designed to explore the role of AA in the coordinate control of growth and defense. We used the *vtc1* and *vtc2* mutants because the slow-growth phenotype observed in these mutants can be reversed by expression of L-gulono-1,4-oxidase, which restores wild-type AA levels and the wild-type phenotype to these mutants (Radzio et al., 2003). These results suggest that low AA alone causes the observed phenotypic characteristics of the *vtc1* and *vtc2* mutants. The results presented in this article allow us to draw the following conclusions.

AA Deficiency Stimulates the Innate Immune Response via Activation of Localized PCD Rather Than Early Senescence

PCD events in plants that can be triggered by elicitors, such as harpin (Boccara et al., 2001), or by pathogens

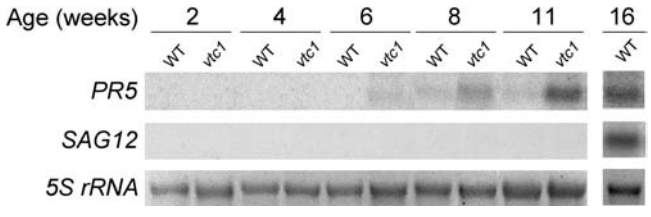

Figure 10. Accumulation of defense-related markers. The abundance of *PR5* and *SAG12* mRNA was determined on RNA blots prepared from naive leaves of 2-, 4-, 6-, 8-, and 11-week-old *vtc1* and wild-type (Col-0) plants. Gel loading was controlled by hybridization with the *5S rRNA* probe.

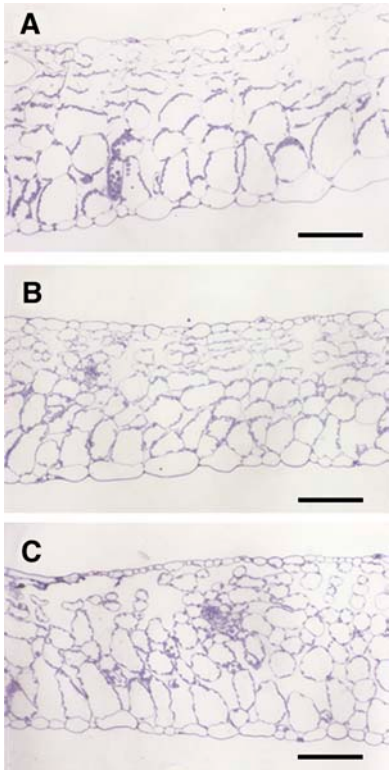

Figure 11. Light microscopy sections of naive leaves showing the comparative cell structure of 10-week-old plants. Wild-type leaves (A) have larger cells than *vtc1* (B) or *vtc2* (C) leaves. Bar, 100 μm.

(Schon et al., 2005) can involve an early loss of photosynthesis and ROS accumulation in chloroplasts (Joo et al., 2005). Moreover, photosynthetic electron transport inhibitors block lesion formation in the lesion mimic mutant (LMM), *lsd1*. Similarly, ROS-mediated lesion development is favored by high light and low CO_2, implicating photorespiratory H_2O_2 production in the PCD response (Mateo et al., 2004). Under optimal growth conditions, photosynthesis is largely unaffected in the *vtc1* and *vtc2* mutants (Pastori et al., 2003). However, photosynthetic CO_2 assimilation and other related parameters are much more sensitive to inhibition by environmental stress and high light in *vtc* mutants compared to the wild type (Mulle-Moule et al., 2002). Here we show AA deficiency limits overall cell size, an effect that becomes apparent only after the first weeks of plant development. Total leaf cell number and size were measured every 2 weeks throughout rosette development. These data show that the wild-type and mutant leaves contain more or less the same number of cells, but that final cell size is smaller in the *vtc1* and *vtc2* mutants than in the wild type. Although leaf AA content is low throughout development, cell area is affected only in older rosettes (age more than 6 weeks; Fig. 12). This result is consistent with known effects of AA on cell wall expansion and cross-linking (Fry, 1998; de Pinto and De Gara, 2004). Interestingly the cessation of growth coincides with the appearance of microscopic lesions (cell death events). Moreover, NPR1 is detectable in the nuclei and key features of SAR appear (*PR* gene expression and increased resistance to virulent pathogens) only after this point, suggesting an inverse correlation between cell growth and activation of innate immune responses.

In Arabidopsis, the age of the leaf is considered to be a predictor of the timing of senescence, the sequential senescence of rosette leaves coinciding with the time of maximum inflorescence development (Hensel et al., 1993). Based on SA accumulation and the early expression of SAGs, Barth et al. (2004) attributed the enhanced pathogen resistance in *vtc* mutants to early senescence. During senescence, leaf metabolism is shifted toward the breakdown of macromolecules, particularly leaf soluble protein and chlorophyll. While the *vtc* mutant leaves accumulate increasing numbers of

Figure 12. The effect of rosette age on cell area in *vtc1* (□), *vtc2* (■), and wild-type (▲) leaves.

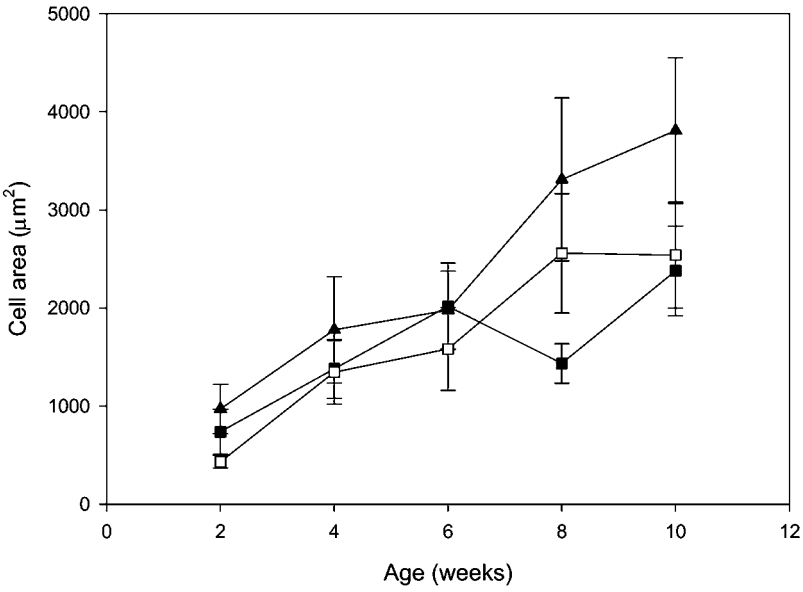

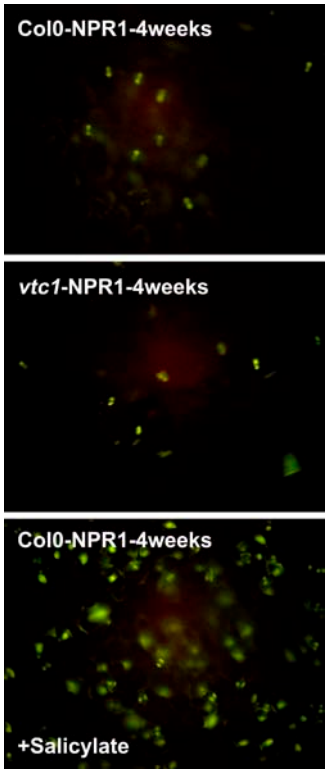

Figure 13. Detection of the cellular localization of GFP fused to NPR1 in transformed 4-week-old wild-type (Col-0-NPR1; top) and *vtc1* plants (*vtc1*-NPR1; middle). Top and middle sections show fluorescence only in stomatal guard cells. The bottom section shows that SA causes fluorescence to appear in mesophyll nuclei as well as in guard cells. The bottom image shows fluorescence in 4-week-old Col-0-NPR1 24 h after spraying with 1 mM SA.

microlesions through development, they do not show early senescence. Evidence supporting this conclusion is as follows: (1) the *vtc* leaves retain chlorophyll and protein longer than those of the wild type; (2) the *vtc* mutants flower later than the wild type; and (3) *SAG12* mRNA was absent at the time when microlesions developed. Taken together, these results confirm that cell death in *vtc* mutants does not result from activation of a senescence program. Since low AA does not trigger early senescence, other effects of AA deficiency must trigger the events leading to enhanced basal resistance.

The data shown in Figure 9 indicate that the expression of H_2O_2-induced genes, such as *GST*, is not constitutively induced in *vtc1*. Moreover, when we analyzed the expression profile of H_2O_2-sensitive genes in *vtc1* using a database search, the *vtc1* transcriptome signature (Pastori et al., 2003) showed no characteristic features of H_2O_2-mediated gene expression (data not shown). Then we compared the effect of AA feeding on the *vtc1* transcriptome (Pastori et al., 2003) with that produced in Arabidopsis cells by H_2O_2 application (Desikan et al., 2001). The data for both the H_2O_2 application (Desikan et al., 2001) and AA feeding microarrays were downloaded from the Stanford Microarray Database (SMD) site and analyzed as described by Desikan et al. (2001) to ensure uniform data analysis, the rationale being that any genes controlled by H_2O_2 in *vtc1* would show reversed expression patterns after AA feeding. AA feeding also modified only 6% of the genes with altered expression patterns following H_2O_2 treatment (Table II). H_2O_2 application led to changes in the expression of 175 expressed sequence tags, of which 113 were induced (26 low expressing, 87 high expressing) and 62 were repressed (Desikan et al., 2001). Of the 106 genes repressed in *vtc1* by AA (Pastori et al., 2003), three of these were also changed by H_2O_2 (two were repressed and one was induced). Of the 112 genes induced by AA (Pastori et al., 2003), Desikan et al. (2001) also reported nine of these, but all were induced. Thus, genes whose expression was modulated by both H_2O_2 and AA showed similar patterns of expression rather than inverse trends. Taking into account effects due to random patterns of gene expression, these results show that the AA and H_2O_2 transcriptome signatures are different, with no common genes with patterns of expression consistent with predicted direct oxidant/antioxidant effects (Table II).

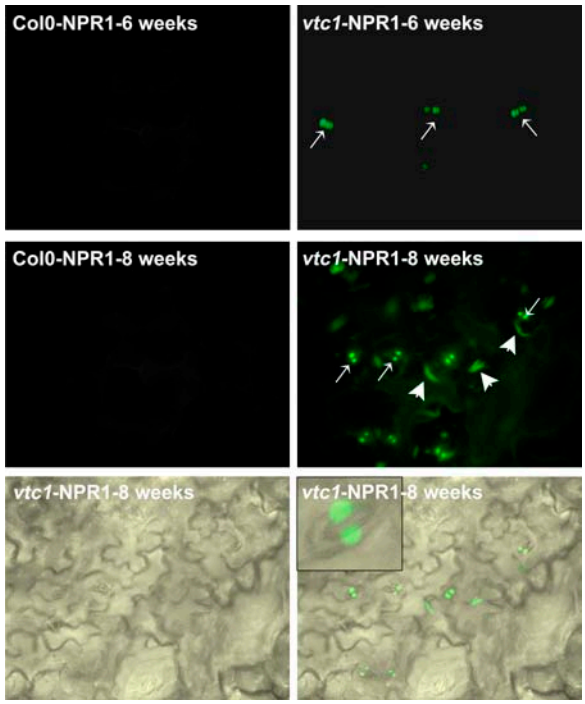

Figure 14. The effect of rosette age on the cellular localization of GFP fused to NPR1 in transformed Col-0 (Col-0-NPR1) and *vtc1* (*vtc1*-NPR1) plants. Fluorescence in the nuclei of mesophyll (arrowheads) and stomatal (fine arrows) guard cells is indicated for leaf samples of 6- and 8-week-old plants. For the *vtc1*-NPR1 8-week-old sample, the bright-field image (bottom left) of the leaves has been overlaid with the GFP fluorescence (bottom right) to illustrate the cellular localization of the fluorescence. The inset shows a higher focus image of an individual stomatal guard cell pair in the epidermis in the overlaid image.

Leaf GSH-to-GSSG Ratios Are Generally Higher in the *vtc* Mutants and This, Together with Low Redox Buffering Capacity, Facilitates SAR Responses

In order to elucidate whether the molecular mechanisms leading to activation of pathogen resistance and SAR responses in the mutants were modulated by altered redox-buffering controls, we first measured the total amount of glutathione and the GSH-to-GSSG ratios in *vtc1*, *vtc2*, and wild-type leaves. The mechanisms through which the SA signal pathway functions are not completely understood, but the ankyrin repeat protein NPR1 is one of the key regulators of SA-dependent gene expression (Cao et al., 1994; Delaney et al., 1995). It has recently been demonstrated that NPR1 is converted from an inactive oligomer to an active monomer as a result of cellular redox changes induced by SA during SAR (Mou et al., 2003). The monomer form of NPR1 moves into the nucleus, where it activates expression of defense genes such as PR1 via redox interaction with TGA transcription factors (Després et al., 2003). Both monomerization of NPR1 oligomers and reduction of monomeric NPR1 involve thiol-disulfide exchange reactions with the participation of glutathione and specific forms of thiol-active proteins, such as thioredoxins, as shown in Figure 1 (Vanacker et al., 2000; Mou et al., 2003; Laloi et al., 2004). The total amount of glutathione and the GSH-to-GSSG ratios were increased in *vtc1* leaves compared to wild-type leaves along development. These data suggest that *vtc1* leaves have key adjustments in the glutathione pool that would favor the monomerization and nuclear translocation of NPR1, resulting in the enhancement of the basal resistance level of the cell. Modulation of cellular glutathione content transmits information through diverse signaling mechanisms, including the establishment of an appropriate redox potential for thiol-disulfide exchange and release of calcium to the cytosol (Gomez et al., 2004). However, the changes in glutathione reported here, since 2 weeks of growth, are not alone sufficient to trigger PR gene expression, which occurs only after 6 to 8 weeks of growth when NPR1 is increasingly located in the nucleus.

The Onset of SAR Is Linked to the Cessation of Expansion Growth and the Appearance of Microlesions But Not to ROS Enhancement in *vtc* Mutants

Our results suggest that another factor associated with low AA is triggered during development and that this, together with favorable GSH-to-GSSG ratios, stimulates SAR. AA deficiency in *vtc1* and *vtc2* activates cell death and the development of microlesions from about 4 weeks and prevents cell expansion from 4 to 6 weeks onward. The onset of SAR is linked in time to the cessation of expansion growth and the appearance of microlesions in *vtc1* and *vtc2*. Nearly 40 Arabidopsis LMMs that develop HR-like lesions on their leaves have been characterized to date. Some, but not all, LMMs develop enhanced disease resistance (Lorrain et al., 2003). Among the LMM mutants having enhanced resistance to virulent infections, *cpn1* (copine), *hrl1* (HR-like lesions), and *hlm1* (HR-like lesion mimic) show low-level or microscopic cell death (Jambunathan et al., 2001; Devadas et al., 2002; Balagué et al., 2003) similar to that observed in *vtc1* leaves. We have found no evidence that *vtc1* and *vtc2* stimulate low-level cell death by ROS enhancement. We conclude that the threshold of sensitivity to ROS produced during the normal course of cell development and growth is decreased because of low redox buffering capacity. Localized ROS accumulation occurs in a wide range of hormone-dependent developmental signaling processes, as well as in cell wall cleavage and associated cell wall growth in a diverse range of developing and expanding organs, such as embryonic axes (Puntarulo and Cederbaum, 1988), roots (Joo et al., 2001; Foreman et al., 2003), germinating seeds (Schopfer et al., 2001), expanding leaves (Rodriguez et al., 2002), and coleoptiles (Schopfer et al., 2002). The absence of apoplastic AA in *vtc1* means that ROS generated during normal developmental signaling will have a longer lifetime than in wild-type plants. In addition, zinc finger proteins and transcription factors involved in PCD and SAR are probably activated in these conditions by virtue of their modulation by cellular redox poise.

In summary, the results demonstrate that AA deficiency positively modulates plant biotic defense cascades leading to greater disease resistance as reported by Barth et al. (2004), but here we show that this effect is not caused by early senescence, as suggested by these authors. In contrast, our results show that *vtc* rosettes exhibit nuclear localization of the NPR1-GFP and SAR in association with localized PCD events. The

Table II. *A comparison of transcripts modulated by ascorbate (A) and H_2O_2 (B)*

Gene Model	A	B	Description of Encoded Protein
At1g49600	−2.4	−1.8	Putative DNA-binding protein (*ACBF*)
At4g14400	−2.4	−2.4	Hypothetical protein
At2g28200	−2.1	+1.6	Zinc finger protein (*ZAT5*)
At3g28200	+1.9	+2.6	Similarity to peroxidase protein
At2g36220	+2.0	+3.9	Unknown proteins
At3g52400	+2.1	+1.9	Syntaxin-like protein (*SYNT4*)
At4g37370	+2.4	+4.2	Cytochrome P450-like protein
At4g39670	+2.4	+3.6	Putative protein
At5g42380	+2.4	+6.9	Similarity to calmodulin
At1g57990	+2.5	+2.2	Similarity to purine permease
At5g59820	+2.5	+8.3	Zinc finger protein (*ZAT12*)
At2g44790	+3.9	+2.2	Phytocyanin II; blue copper-binding protein II

observed overall smaller leaf cell size in the *vtc* leaves is consistent with the known roles of AA in cell wall formation. However, this cannot be the sole explanation of the smaller cell area in the *vtc* lines because cell expansion is affected only in older rosettes, even though AA content is low throughout leaf development. It is possible that AA levels also modulate DELLA protein activity and hence growth by modulation of gibberellic acid and abscisic acid levels, as discussed previously (Pastori et al., 2003). The inverse relationship between growth and defense that is frequently observed in plants is crucial in any consideration of plant productivity, but it is poorly understood. The results presented suggest that cellular AA may be one component that influences this relationship acting either downstream or alongside ROS accumulation to coordinate plant growth and defense processes.

MATERIALS AND METHODS

Plant Growth

Seeds of the wild-type Arabidopsis (*Arabidopsis thaliana* L. Heynh. accession Col-0) and the *vtc1-1* and *vtc2-2* mutants were obtained from the Nottingham Arabidopsis Stock Centre (NASC) and from Nick Smirnoff (University of Exeter). These plants were grown in a controlled environment chamber essentially as described previously (Veljovic-Jovanovic et al., 2001). Plants were grown for 12 weeks at 22°C under low (250 μmol m^{-2} s^{-1}) light with a 10-h photoperiod and 70% humidity. The air in the chamber was filtered to remove atmospheric ozone and with strict hygiene.

Biomass, Chlorophyll, and Metabolite Analyses

Whole rosettes were harvested in the growth chamber and biomass recorded (fresh weight). Extraction and assay of AA, glutathione, protein, and chlorophyll were performed as described previously (Vernon, 1960; Veljovic-Jovanovic et al., 2001).

Pathogen Inoculation

The virulent *Pseudomonas syringae* pv tomato strain DC3000 (*Pst*) was grown overnight in King's B medium with 10 μg/mL tetracycline and 100 μg/mL rifampicine, and bacterial suspensions were washed twice in 10 mM $MgCl_2$, diluted to appropriate concentrations and used for infiltration into fully expanded leaves at two sites on the abaxial surface, as previously described (Alvarez et al., 1998). For bacterial growth curves, two leaf discs (6-mm diameter) were cut around the *Pst*-inoculation sites from each leaf. Discs from different inoculated leaves were pooled at each time point and homogenized in 10 mM $MgCl_2$ to liberate the bacteria. Serial dilutions of the homogenates were plated (in duplicate) on King's B medium supplemented with 10 μg/mL tetracycline and 100 μg/mL rifampicine. Colonies on the plates were counted after incubation at 28°C for 24 h.

Northern-Blot Analysis

Total RNA was prepared for RNA gel-blot hybridization analysis by use of standard protocols as described previously (Alvarez et al., 1998). Arabidopsis probe templates were used for detection of *GST-1* (At1g02930), *SAG12* (At5g45890), *PR-1* (At2g14610), *PR-2* (At3g57260), and *PR-5* (At1g75040) transcripts (Uknes et al., 1992).

Plant Transformation

Competent *Agrobacterium tumefaciens* (strain GV3101; pMP90) were prepared using the protocol of McCormac et al. (1998). Arabidopsis (Col-0/*vtc1*) plants were transformed with Agrobacterium containing the NPR1-GFP construct (pBI 1.4t backbone; Kinkema et al., 2000) using a simple dip transformation technique (Clough and Bent, 1998). Primary transformed seedlings were selected on Murashige and Skoog agar plates containing kanamycin (2.1 g/L Murashige and Skoog salts, 0.7% bacto-agar, and 50 μg/mL kanamycin, pH 5.7).

Microscopy

GFP fluorescence in leaves expressing the NPR1 reporter constructs was determined using a Zeiss Axiophot microscope. Leaf samples were mounted in water and illuminated using an excitation and emission wavelength of 490 and 510 nm, respectively, and viewed using the appropriate filters (BP 470/20, FT 493, BP 505–530; Zeiss).

Histochemistry

Leaf sections were fixed and embedded in Spurr's medium as described by Jones et al. (2002). Semithin sections (0.5 μm) were stained with toluidine blue and examined with a Leica DMR light microscope. Quantitative determinations were developed using an imaging analysis Leica QM500 as described previously by Olmos and Hellín (1998).

Dead cells were identified using lactophenol blue (Fluka) staining followed by destaining in saturated chloral hydrate as previously described (Waspi et al., 2001). Leaves were then mounted on microscopic slides in 40% glycerol and analyzed by bright-field or blue-light incident fluorescence microscopy. Numbers of dead cells per leaf were counted and 40 independent measurements were made per time point. Autofluorescence detection was performed as described previously (Waspi et al., 2001).

ACKNOWLEDGMENT

We thank Xinnian Dong for the generous gift of the NPR1-GFP construct.

Received June 28, 2005; revised August 12, 2005; accepted August 12, 2005; published October 21, 2005.

LITERATURE CITED

Alvarez ME, Pennell RI, Meijer PJ, Ishikawa A, Dixon RA, Lamb C (1998) Reactive oxygen intermediates mediate a systemic signal network in the establishment of plant immunity. Cell **20:** 773–784

Apel K, Hirt H (2004) Reactive oxygen species: metabolism, oxidative stress, and signal transduction. Annu Rev Plant Physiol Plant Mol Biol **55:** 373–399

Arrigoni O, de Tullio MC (2000) The role of ascorbic acid in cell metabolism: between gene-directed functions and unpredictable chemical reactions. J Plant Physiol **157:** 481–488

Balagué C, Lin B, Alcon C, Flottes G, Malmstrom S, Kohler C, Neuhaus G, Pelletier G, Gaymard F, Roby D (2003) HLM1, an essential signaling component in the hypersensitive response, is a member of the cyclic nucleotide-gated channel ion channel family. Plant Cell **15:** 365–379

Barth C, Moeder W, Klessig DF, Conklin PL (2004) The timing of senescence and response to pathogens is altered in ascorbate-deficient mutant vitamin C-1. Plant Physiol **134:** 178–192

Boccara M, Boue C, Garmier M, De Paepe R, Boccara AC (2001) Infra-red thermography revealed a role for mitochondria in pre-symptomatic cooling during harpin-induced hypersensitive response. Plant J **28:** 663–670

Cameron R, Dixon RA, Lamb CJ (1994) Biologically induced systemic acquired resistance in *Arabidopsis thaliana*. Plant J **5:** 715–725

Cao H, Bowling SA, Gordon S, Dong X (1994) Characterization of an Arabidopsis mutant that is non-responsive to inducers of systemic acquired resistance. Plant Cell **6:** 1583–1592

Chamnongpol S, Willekens H, Langebartels C, Van Montagu M, Inze D, Van Camp W (1996) Transgenic tobacco with a reduced catalase activity develops necrotic lesions and induces pathogenesis-related expression under high light. Plant J **10:** 491–503

Chen C, Dickman MB (2004) Bcl-2 family members localize to tobacco chloroplasts and inhibit programmed cell death induced by chloroplast-targeted herbicides. J Exp Bot **55:** 2617–2623

Clough SJ, Bent AF (1998) Floral dip: a simplified method for Agrobacterium-mediated transformation of *Arabidopsis thaliana.* Plant J **16:** 735–743

Conklin PL, Norris SR, Wheeler GL, Williams EH, Smirnoff N, Last RL (1999) Genetic evidence for the role of GDP-mannose in plant ascorbic acid (vitamin C) biosynthesis. Proc Natl Acad Sci USA **30:** 4198–4203

Conklin PL, Williams EH, Last RL (1996) Environmental stress sensitivity of an ascorbic acid-deficient Arabidopsis mutant. Proc Natl Acad Sci USA **3:** 9970–9974

Conklin PL, Saracco SA, Norris SR, Last RL (2000) Identification of ascorbic acid deficient *Arabidopsis thaliana* mutants. Genetics **154:** 847–856

Delaney TP, Friedrich L, Ryals JA (1995) Arabidopsis signal transduction mutant defective in chemically and biologically induced disease resistance. Proc Natl Acad Sci USA **92:** 6602–6606

Delledonne M, Zeier J, Marocco A, Lamb C (2001) Signal interactions between nitric oxide and reactive oxygen intermediates in the plant hypersensitive disease resistance response. Proc Natl Acad Sci USA **98:** 13454–13459

de Pinto MC, De Gara L (2004) Changes in the ascorbate metabolism of apoplastic and symplastic spaces are associated with cell differentiation. J Exp Bot **55:** 2559–2569

Desikan R, A-H-Mackerness S, Hancock JT, Neill SJ (2001) Regulation of the Arabidopsis transcriptome by oxidative stress. Plant Physiol **127:** 159–172

Després C, Chubak C, Rochon A, Clark R, Bethune T, Desveaux D, Fobert PR (2003) The Arabidopsis NPR1 disease resistance protein is a novel cofactor that confers redox regulation of DNA binding activity to the basic domain/leucine zipper transcription factor TGA1. Plant Cell **15:** 2181–2191

Devadas SK, Enyedi A, Raina R (2002) The *Arabidopsis hrl1* mutation reveals novel overlapping roles for salicylic acid, jasmonic acid and ethylene signalling in cell death and defence against pathogens. Plant J **30:** 467–480

Foreman J, Demidchik V, Bothwell JH, Mylona P, Miedema H, Torres MA, Linstead P, Costa S, Brownlee C, Jones JD, et al (2003) Reactive oxygen species produced by NADPH oxidase regulate plant cell growth. Nature **422:** 442–446

Foyer CH (2004) The role of ascorbic acid in defence networks and signalling in plants. *In* H Asard, JM May, N Smirnoff, eds, Vitamin C. Functions and Biochemistry in Animals and Plants. BIOS Scientific Publishers, Oxon, UK, pp 65–82

Foyer CH, Noctor G (2005a) Redox homeostasis and antioxidant signalling: a metabolic interface between stress perception and physiological responses. Plant Cell **17:** 1866–1875

Foyer CH, Noctor G (2005b) Oxidant and antioxidant signalling in plants: a re-evaluation of the concept of oxidative stress in a physiological context. Plant Cell Environ **28:** 1056–1071

Fry SC (1998) Oxidative scission of plant cell wall polysaccharides by ascorbate-induced hydroxyl radicals. Biochem J **332:** 507–515

Gomez LD, Noctor G, Knight MR, Foyer CH (2004) Regulation of calcium signalling and gene expression by glutathione. J Exp Bot **55:** 1851–1859

Green R, Fluhr R (1995) UV-B-induced PR-1 accumulation is mediated by active oxygen species. Plant Cell **7:** 203–212

Hensel LL, Grbic V, Baumgarten DA, Bleecker AB (1993) Developmental and age-related processes that influence the longevity and senescence of photosynthetic tissues in Arabidopsis. Plant Cell **5:** 553–564

Jabs T, Dietrich RA, Dangl JL (1996) Initiation of runaway cell death in an *Arabidopsis* mutant by extracellular superoxide. Science **273:** 1853–1856

Jambunathan N, Siani JM, McNellis TW (2001) A humidity-sensitive Arabidopsis copine mutant exhibits precocious cell death and increased disease resistance. Plant Cell **13:** 2225–2240

Jones B, Frasse P, Olmos E, Zegzouti H, Leclerq J, Tournier B, Latché A, Pech JC, Bouzayen M (2002) Down-regulation of DR12, an auxin-response-factor homolog, in the tomato results in pleiotropic phenotype including dark-green and blotchy ripening fruit. Plant J **32:** 603–613

Joo JH, Bae YS, Lee JS (2001) Role of auxin-induced reactive oxygen species in root gravitropism. Plant Physiol **126:** 1055–1060

Joo JH, Wang S, Chen JG, Jones AM, Fedoroff NV (2005) Different signalling and cell death roles of heterotrimeric G protein a and b subunits in the Arabidopsis oxidative stress response to ozone. Plant Cell **17:** 957–970

Kiddle G, Pastori GM, Bernard B, Pignocchi C, Antoniw J, Verrier PJ, Foyer CH (2003) Effects of leaf ascorbate content on defense and photosynthesis gene expression in *Arabidopsis thaliana.* Antioxid Redox Signal **5:** 23–32

Kinkema M, Fan W, Dong X (2000) Nuclear localisation of NPR1 is required for activation of PR gene expression. Plant Cell **12:** 2339–2350

Laloi C, Apel K, Danon A (2004) Reactive oxygen signalling: the latest news. Curr Opin Plant Biol **7:** 323–328

Levine A, Pennell RI, Alvarez ME, Palmer R, Lamb C (1996) Calcium-mediated apoptosis in a plant hypersensitive disease resistance response. Curr Biol **6:** 427–437

Lorrain S, Vailleau F, Balague C, Roby D (2003) Lesion mimic mutants: keys for deciphering cell death and defense pathways in plants? Trends Plant Sci **8:** 263–271

Mateo A, Mühlenbock P, Rustérucci C, Chang CCC, Miszalski Z, Karpinska B, Parker JE, Mullineaux PM, Karpinski S (2004) *LESION SIMULATING DISEASE 1* is required for acclimation to conditions that promote excess excitation energy. Plant Physiol **136:** 2818–2830

Matsumura H, Nirasawa S, Kiba A, Urasaki N, Saitoh H, Ito M, Kawai-Yamada M, Uchimiya H, Terauchi R (2003) Overexpression of Bax inhibitor suppresses the fungal elicitor-induced cell death in rice (Oryza sativa L) cells. Plant J **33:** 425–434

Maxwell DP, Nickels R, McIntosh L (2002) Evidence of mitochondrial involvement in the transduction of signals required for the induction of genes associated with pathogen attack and senescence. Plant J **29:** 269–279

McCormac AC, Elliott MC, Chen DF (1998) A simple method for the production of highly competent cells of Agrobacterium for transformation via electroporation. Mol Biotechnol **9:** 155–159

Mou Z, Fan W, Dong X (2003) Inducers of plant systemic acquired resistance regulate NPR1 function through redox changes. Cell **27:** 935–944

Mulle-Moule P, Conklin PL, Niyogi KK (2002) Ascorbate deficiency can limit violaxanthin de-epoxidase activity in vivo. Plant Physiol **128:** 970–977

Navabpour S, Morris K, Allen R, Harrison E, A-H-Mackerness S, Buchanan-Wollaston V (2003) Expression of senescence-enhanced genes in response to oxidative stress. J Exp Bot **54:** 2285–2292

Noctor G, Foyer CH (1998) Ascorbate and glutathione: keeping active oxygen under control. Annu Rev Plant Physiol Plant Mol Biol **49:** 249–279

Noctor G, Gomez L, Vanacker H, Foyer CH (2002) Interactions between biosynthesis, compartmentation and transport in the control of glutathione homeostasis and signalling. J Exp Bot **53:** 1283–1304

Olmos E, Hellín E (1998) Ultrastructural differences of hyperhydric and normal leaves from regenerated carnation plants. Sci Hortic (Amsterdam) **75:** 91–101

Pastori GM, Kiddle G, Antoniw J, Bernard S, Veljovic-Jovanovic S, Verrier PJ, Noctor G, Foyer CH (2003) Leaf vitamin C contents modulate plant defense transcripts and regulate genes controlling development through hormone signaling. Plant Cell **15:** 939–951

Potters G, De Gara L, Asard H, Horemans N (2002) Ascorbate and glutathione: guardians of the cell cycle, partners in crime? Plant Physiol Biochem **40:** 537–548

Potters G, Horemans N, Bellone S, Caubergs RJ, Trost P, Guisez Y, Asard H (2004) Dehydroascorbate influences the plant cell cycle through a glutathione-independent reduction mechanism. Plant Physiol **134:** 1479–1487

Puntarulo S, Cederbaum AI (1988) Comparison of the ability of ferric complexes to catalyze microsomal chemiluminescence, lipid peroxidation, and hydroxyl radical generation. Arch Biochem Biophys **264:** 482–491

Radzio A, Lorence A, Chevone BI, Nessler CL (2003) L-Gulono-1,4-lactone oxidase expression rescues vitamin C-deficient Arabidopsis (*vtc*) mutants. Plant Mol Biol **53:** 837–844

Rodriguez AA, Grunberg KA, Taleisnik EL (2002) Reactive oxygen species in the elongation zone of maize leaves are necessary for leaf extension. Plant Physiol **129:** 1627–1632

Schon P, Degefa TH, Asaftei S, Meyer W, Walder L (2005) Charge propagation in ''ion channel sensors'' based on protein-modified electrodes and redox marker ions. J Am Chem Soc **127:** 11486–11496

Schopfer P, Liszkay A, Bechtold M, Frahry G, Wagner A (2002) Evidence that hydroxyl radicals mediate auxin-induced extension growth. Planta **214:** 821–828

Schopfer P, Plachy C, Frahry G (2001) Release of reactive oxygen intermediates (superoxide radicals, hydrogen peroxide, and hydroxyl radicals) and peroxidase in germinating radish seeds controlled by light, gibberellin, and abscisic acid. Plant Physiol **125:** 1591–1602

Thomas H, Ougham HJ, Wagstaff C, Stead AD (2003) Defining senescence and death. J Exp Bot **54:** 1127–1132

Tokuna T, Miyahara K, Tabata K, Esaka M (2005) Generation and properties of ascorbic acid-over-producing transgenic tobacco cells expressing sense RNA for L-galactono-1,4-lactone dehydrogenase. Planta **220:** 854–863

Uknes S, Mauch-Mani B, Moyer M, Potter S, Williams S, Dincher S, Chandler D, Slusarenko A, Ward E, Ryals J (1992) Acquired resistance in Arabidopsis. Plant Cell **4:** 645–656

Vanacker H, Carver TL, Foyer CH (2000) Early H_2O_2 accumulation in mesophyll cells leads to induction of glutathione during the hyper-sensitive response in the barley-powdery mildew interaction. Plant Physiol **123:** 1289–1300

Veljovic-Jovanovic SD, Pignocchi C, Noctor G, Foyer CH (2001) Low ascorbic acid in the *vtc-1* mutant of Arabidopsis is associated with decreased growth and intracellular redistribution of the antioxidant system. Plant Physiol **127:** 426–435

Vernon LP (1960) Spectrophotometric determination of chlorophylls and pheo-phytins in plant extracts. Anal Chem **32:** 1144–1150

Wagner D, Przybyla D, Op den Camp R, Kim C, Landgraf F, Lee KP, Würsch M, Laloi C, Nater M, Hideg E, et al (2004) The genetic basis of singlet oxygen-induced stress responses of *Arabidopsis thaliana*. Science **306:** 1183–1185

Waspi U, Schweizer P, Dudler R (2001) Syringolin reprograms wheat to undergo hypersensitive cell death in a compatible interaction with powdery mildew. Plant Cell **13:** 153–161

Whalen MC, Innes RW, Bent AF, Staskawicz BJ (1991) Identification of *Pseudomonas syringae* pathogens of Arabidopsis and a bacterial locus determining avirulence on both Arabidopsis and soybean. Plant Cell **3:** 49–59

Yao N, Eisfelder BJ, Marvin J, Greenberg JT (2004) The mitochondrion—an organelle commonly involved in programmed cell death in *Arabidopsis thaliana*. Plant J **40:** 596–610